

From microscopic to macroscopic dynamics in mean-field theory: effect of neutron skin on fusion barrier and dissipation.

Denis Lacroix

LPC/ISMRA, Blvd du Maréchal Juin, 14050 Caen, France

In this work, we introduce a new method to reduce the microscopic mean-field theory to a classical macroscopic dynamics during the initial stage of fusion reactions. We show that TDHF (Time-dependent Hartree-Fock) could be a useful tool to gain information on fusion barriers as well as on one-body dissipation effects. We apply the mean-field theory to the case of head-on reaction between ^{16}O and $^{16,22,24,28}\text{O}$ in order to quantify the effect of neutron skin on fusion. We show that the determination of fusion barrier requires, in addition to a precise knowledge of the relative distance between the center of mass of the two fusing nuclei, the introduction of an additional collective coordinate that explicitly breaks the neutron-proton symmetry. In this context, we estimate the position, height and diffuseness of the barrier as well as the one-body friction and show that a global enhancement of the fusion cross-section is expected in neutron rich nuclei.

(November 5, 2018)

PACS: 21.60.Jz, 24.10.-i, 25.60.Pj

Keywords: mean-field, fusion reactions , neutron skin.

I. INTRODUCTION

The understanding of the formation of compact system during fusion of two nuclei implies the development of nuclear models which can take into account quantum effects, the dynamical evolution and dissipation in a common framework. From that point of view, the description of the conversion of relative motion into internal excitation of the composite system and also the deexcitation of the compound nucleus is far from being complete. Due to the diversity of dissipative mechanisms, the microscopic descriptions of fusion reactions is often substituted by a macroscopic dynamics in which only few relevant degrees of freedom are considered. Such macroscopic description are only valid under a series of assumption like separation in time-scales between relevant and other degrees of freedom. The validity of these hypothesis as well as the link with microscopic theories is under debate.

In the present work, starting from quantum mean-field theory, we address the problem of the reduction of the microscopic dynamics to a macroscopic theory [1–5].

A. Mean-field theories

We consider the Time-Dependent Hartree-Fock (TDHF) theory: one-body degrees of freedom are supposed to be dominant and the description of the system reduces to the time evolution of a Slater-determinant $|\Psi\rangle$ in a self-consistent mean-field. Noting ρ the associated one-body density matrix, the evolution is given by the Liouville equation [6]

$$i\hbar \frac{d\rho}{dt} = [h[\rho], \rho] \quad (1)$$

where $h[\rho]$ is the self-consistent field. Such a picture has been widely used to investigate nuclear dissipative reac-

tions, and gives reasonable results in the case of fusion reactions [7–9]. In addition, it has the advantage to take into account shell effects and to include the so-called one-body dissipation.

However, fusion reactions and more generally deep inelastic reactions are often described assuming that some macroscopic variables are dominant [2,10]. Although a large number of work is devoted to this subject, the link between macroscopic dynamics and microscopic approaches such as TDHF is still unclear [11].

In this paper, we address this problem considering head-on reactions. In this case, the relative distance R between nuclei in the entrance channel is known to describe the main features of the dynamics and its evolution follows the classical Hamilton-like equation * [3]:

$$\begin{cases} \frac{dR}{dt} = P/\mu(R) \\ \frac{dP}{dt} = F(R) - \gamma(R)\dot{R} \end{cases} \quad (2)$$

where $\mu(R)$ is the reduced mass of the system and the force is assumed to derive from a potential ($F(R) = -\frac{\partial V}{\partial R}$). The dissipation kernel $\gamma(R)$ is supposed to reproduce the effect of the other non described degrees of freedom on the considered variables.

The dissipative effects are generally taken by including the one-body dissipation in a liquid drop picture [13] or using an adiabatic approximation in a two-center shell model (see for instance [14]). However, the understanding of dissipative effects in nuclear collisions is far from

*For simplicity, we have written the expression in its simplest form, it should however be noted that other degrees of freedom like angular momentum [3] or mass asymmetry [12] may be considered in the formalism.

being complete and the use of equation (2) rises some questions. A large number of effects are known to participate to the dissipation of the relative to the internal excitation energy during the reaction. Among them, exchange of particles and deformation are generally assumed to be dominant and are accounted as one-body dissipation effects. We would like however to mention that the dissipative process described by equation (2) is obtained using quantum perturbation theory [15]. It is not clear whether it can be applied to the case of violent collisions like fusion.

Mean-field theory like TDHF does a priori includes one-body dissipation in a non-perturbative framework. In addition, it assume neither separation between degrees of freedom nor adiabaticity. However, the link with the so-called one-body dissipation theory is still under discussion [16].

It should also be noted that friction models assumes a fast equilibration of other degrees of freedom as compared to the relative motion leading to the formation of a compound nucleus at finite temperature. Due to the absence of two-body or higher order correlations, TDHF is unable to account for this effect. From the experimental point of view, the equilibration time is estimated to be of the order of the reaction time [17], which means that the classical description assuming thermal equilibration assumption is questionable as far as fusion is concerned.

In this paper, we discuss the possibility to use macroscopic equations for TDHF although it does not assume perturbation theory or equilibration. In the following, we show that such a reduction seems possible and gives reasonable results on fusion barriers properties.

Different works already exist on the possibility of such a reduction of microscopic theory [18,25–27]. However, as it was already noted in [18], high numerical accuracy as well as the use of complete realistic effective forces is required. In this article, we use the three-dimensional TDHF code developed by Bonche and co-workers [19] and the full SLy4d Skyrme force including spin-orbit [20].

In the following, we apply the mean-field theory to head-on reactions between oxygen isotopes. The static properties of oxygen isotopes are first presented. We then describe the method used to reduce mean-field evolution to the relative distance only and extract quantitative information on the fusion process. The macroscopic potential landscape and the dissipative aspects are then discussed.

II. RESULTS

A. Structure of oxygen isotopes

For each of the considered nuclei, the self-consistent Hartree-Fock equation reads:

$$h[\rho] |\varphi_i^\tau\rangle = \epsilon_i |\varphi_i^\tau\rangle, \quad (3)$$

where $h[\rho]$ is the mean-field hamiltonian, $|\varphi_i^\tau\rangle$ denotes the single particle wave functions and τ denotes the isospin quantum number ($\tau = p$ [proton] or $\tau = n$ [neutron]). Equation 3 is solved in r-space on a mesh of size $(16 fm)^3$ with a step of 0.8 fm. The complete expression of $h[\rho]$ for Skyrme forces can be found for instance in [21]. The resulting single-particle levels energies obtained using the SLy4d Skyrme force are presented in Fig. 1 for the four isotopes ^{16}O , ^{22}O , ^{24}O and ^{28}O .

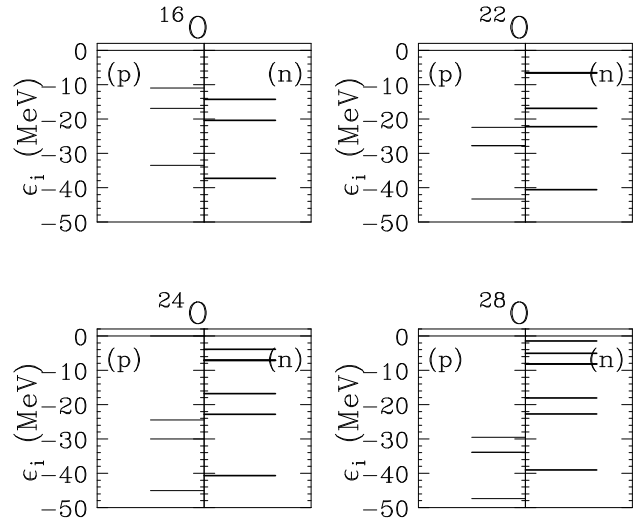


FIG. 1. Proton (p) and neutrons (n) energy levels obtained in Hartree-Fock calculation described in the text using the SLy4d effective Skyrme force for ^{16}O , ^{22}O , ^{24}O , ^{28}O isotopes.

The associated neutron and proton root mean square radius (RMS) are reported in figure 2. These root mean square radii leads to RMS matter radii in agreement with experimental data for the ^{16}O , ^{22}O and ^{24}O nuclei [28]. A neutron skin is evidenced when the number of neutrons increases.

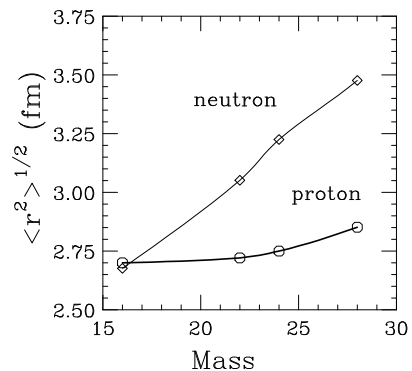


FIG. 2. Proton (circle) and neutron (diamond) root mean square radius predicted by the Hartree-Fock calculation using the SLy4d Skyrme interaction for the ^{16}O , ^{22}O , ^{24}O , ^{28}O isotopes.

Once the static properties are obtained, we consider

the evolution of the two colliding nuclei in a larger volume $(32fm)^3$ with the same step in r-space as before. The initial distance between the center of the two nuclei is equal to 16 fm. The time step is chosen as 0.45 fm/c. Before showing the results of the dynamical calculation, we discuss the method used to reduce the mean-field dynamics to the time evolution of a few macroscopic coordinates.

B. Reduction to macroscopic dynamics

In order to define the relative distance between the two nuclei, we consider the mean-field equation in r-space and the associated one-body density $\rho^\tau(r, r')$ with $\rho^\tau = \sum_i |\varphi_i^\tau(t)\rangle \langle \varphi_i^\tau(t)|$. We assume, as in ref. [23], that at each time step, the system could be split into two subspaces 1 and 2 with the associated densities ρ_x^τ ($x = 1, 2$). We define the separation plane after the contact at the neck position as it is done generally in macroscopic models [22].

Once the separation is obtained, we compute for each subspace, the number of neutrons $N_x = Tr(\rho_x^n)$ or protons $Z_x = Tr(\rho_x^p)$, the mean position

$$R_x^\tau \equiv \langle \hat{r} \rangle_x = Tr(\hat{r}\rho_x^\tau) / Tr(\rho_x^\tau) \quad (4)$$

and the associated momentum

$$P_x^\tau \equiv \langle \hat{p} \rangle_x = Tr(\hat{p}\rho_x^\tau) \quad (5)$$

where Tr denotes the Trace. Let us first assume that we can neglect the isospin degree of freedom (the validity of this assumption will be discussed in the following). We define the center of mass as well as the associated total momentum:

$$R_x = (N_x R_x^n + Z_x R_x^p) / A_x \quad (6)$$

$$P_x = P_x^n + P_x^p. \quad (7)$$

where we have introduced $A_x = N_x + Z_x$.

Using Hamilton equation for each subsystem, we estimate the mass from equation 2

$$m_x = P_x / \left(\frac{dR_x}{dt} \right) \quad (8)$$

At a given relative distance $R = R_1 - R_2$, we compute the reduced mass associated with the composite system $\mu(R) = m_1 m_2 / (m_1 + m_2)$. Note that, since we have a Skyrme force, with in particular t_1 , t_2 and spin-orbit terms, $\mu(R)$ is different from the normal value:

$$\mu_0(R) = m \frac{A_1(R) A_2(R)}{(A_1(R) + A_2(R))} \quad (9)$$

where m is the nucleon mass. In our calculation, we obtain $\mu(R)/\mu_0(R) \simeq cte \simeq 0.67$ for all systems. This remains valid up to the formation of a compact shape.

Once these quantities have been defined and calculated, the different components entering in Eq. (2): $R(t)$, $dR(t)/dt$, $P(t)$ and its derivative can be computed.

Eq. 2 contains two unknown quantities, the force $F(R)$ and the friction coefficient $\gamma(R)$. In order to estimate these quantities, a method proposed in ref. [24,18] is used. It consists in performing mean-field evolution with two slightly different initial energies E^I , E^{II} . At a given position R , Eq. 2 can be interpreted as a system of two equations with two unknown quantities which reads:

$$\begin{pmatrix} 1 & -\frac{dR^I}{dt} \\ 1 & -\frac{dR^{II}}{dt} \end{pmatrix} \begin{pmatrix} F(R) \\ \gamma(R) \end{pmatrix} = \begin{pmatrix} \frac{dP^I}{dt} \\ \frac{dP^{II}}{dt} \end{pmatrix} \quad (10)$$

where all derivatives are taken at position R . We checked the numerical stability of the proposed procedure, by solving the classical equation associated with the same initial condition as TDHF evolution and with the friction and potential extracted from it. As expected, we recover the TDHF evolution.

C. Nuclear potential

We performed TDHF calculations with four different initial center of mass energies $E/A = 0.60, 0.65, 0.70$ and 0.75 MeV for each reaction. Figure 3 gives the potential for the reactions $^{16}\text{O} + ^{16,22,24,28}\text{O}$ obtained by inversion of Eq. 10. To extract the nuclear part, we assume $V_{nuclear}(R) = V(R) - V_C(R)$, where the coulomb part is simply taken as $V_C(R) = e^2 Z_1(R) Z_2(R) / R$ (dashed line). For each reaction, we have solved Eq. 10 using different couple of TDHF evolution with different initial energies. The solution depends slightly on the couple of trajectories chosen, this uncertainty is represented by errorbars in Fig. 3. The uncertainties are rather small indicating that the microscopic dynamics is already well described by Eq. 2.

Examining the global shape of $V(R)$, and in particular the maximum, we see that although the barrier height is slightly affected by the neutron skin, the increase of the neutron number not only increases the barrier position R_B but also change its diffuseness. This effect should normally indicate a very different behavior in the sub-barrier fusion of very neutron rich nuclei as compared to stable isotopes. Using a different technique, the same conclusion is drawn in ref. [29] while in ref. [30,19], it is concluded that the excess of neutron does not affect fusion. This point is discussed in the following

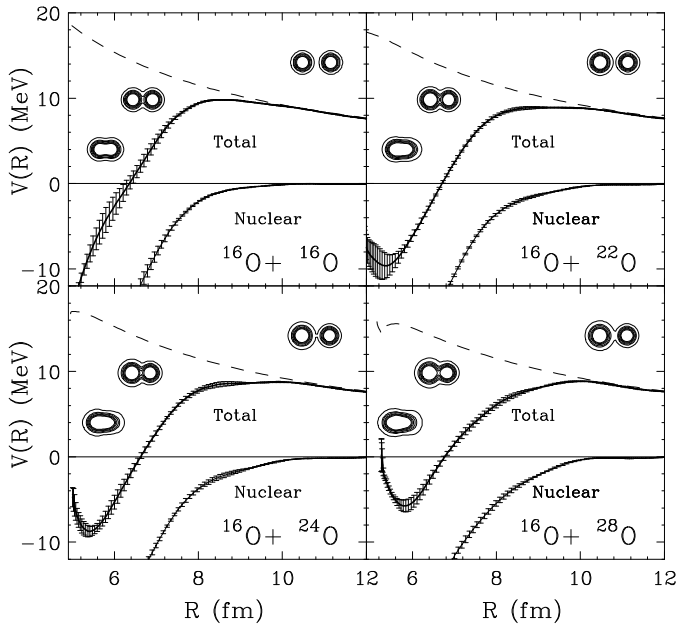


FIG. 3. Potential landscape obtained in head-on $^{16}\text{O}+^{16,22,24,28}\text{O}$ reactions. The total (thick solid lines), coulomb (dashed line) and nuclear potential (thin solid lines) are presented. For the calculation, different couples of trajectories taken within the initial energies $E/A = 0.75, 0.70, 0.65, 0.60$ MeV are presented. "Errorbars" correspond to the mean-variance on results obtained with different initial conditions. The isodensity plots in the reaction plane are also superimposed for different times.

D. Dissipation

While numerous works have been devoted to potentials determination, only few quantitative analyses exist on the dissipation effects starting from a non-adiabatic microscopic theory. The method described above gives also information on the dissipative processes. The friction coefficient associated to the mean-field evolution of the system can be computed. It is presented in Fig. 4.

In order to have a global information on the amount of energy transferred from the relative motion into internal degrees of freedom of the compound system, the integrated value of the Rayleigh function can be evaluated. The Rayleigh function gives the rate of energy dissipated by unit of time:

$$E_{ray}(t) = dE/dt = -\gamma(R)\dot{R}^2 \quad (11)$$

and its integrated value $E_{loss}(R(t))$ reads (Fig. 4):

$$E_{loss}(t) = 2 \int_{t_0}^t E_{ray}(s) ds \quad (12)$$

In order to compare different systems, $\gamma(R)$ and $E_{loss}(R(t))$ are plotted as a function of the relative distance normalized to $R_{12} = \frac{5}{3} (\langle r_T^2 \rangle^{1/2} + \langle r_P^2 \rangle^{1/2})$ where P and T refers respectively to the projectile and target. It is worth noticing that dissipation is larger at larger distances than $R/R_{12} \sim 0.7$ in the case of neutron rich nuclei. However, at intermediate distance $0.5 < R/R_{12} < 0.7$ the dissipation is larger in the symmetric case. We indeed expect a different behavior between symmetric and asymmetric systems. If the one-body dissipation picture is correct, part of the viscosity is due to the change of the global shape of the system (the so-called wall dissipation [31]). In asymmetric reactions, this effect should be completed by the friction due to the exchange of nucleons between the two subsystems (the window dissipation [32]). The link between the friction coefficient in TDHF and the wall plus window picture is however not clear. Indeed, mean-field theory also includes other degrees of freedom which are not taken into account in the wall and window formula. In particular, a fraction of the initial energy is converted into collective excitation (giant resonances). In our case, this effect is also integrated in $\gamma(R)$.

We finally would like to mention that, although the dissipation is different between symmetric and asymmetric systems, the value of E_{loss} at minimal distance of approach is independent of the asymmetry.

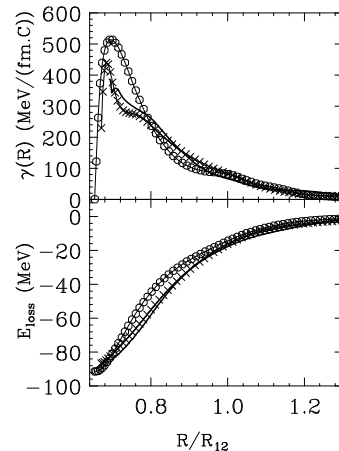


FIG. 4. Top: Friction coefficient as a function of relative distance of head-on $^{16}\text{O}+^{16}\text{O}$ (circles), $^{16}\text{O}+^{22}\text{O}$ (crosses) and $^{16}\text{O}+^{28}\text{O}$ (thick lines) reactions. Bottom: Associated integrated Rayleigh function E_{loss} as a function of the relative distance normalized to the sum of the nuclear radius of the target and projectile $R_{12} = \sqrt{\frac{5}{3}} (\langle r_T^2 \rangle^{1/2} + \langle r_P^2 \rangle^{1/2})$. In these figures errorbars are not shown. For simplicity, we do not show the $^{16}\text{O}+^{24}\text{O}$ which is similar to the $^{16}\text{O}+^{22}\text{O}$ case.

E. Precise determination of the barrier properties

The possibility to obtain fusion cross-section from mean-field requires a precise estimate of the nuclear po-

tential in the vicinity of the fusion barrier. Details of the fusion barrier extracted using Eq. 2 are shown in figure 5 (gray area).

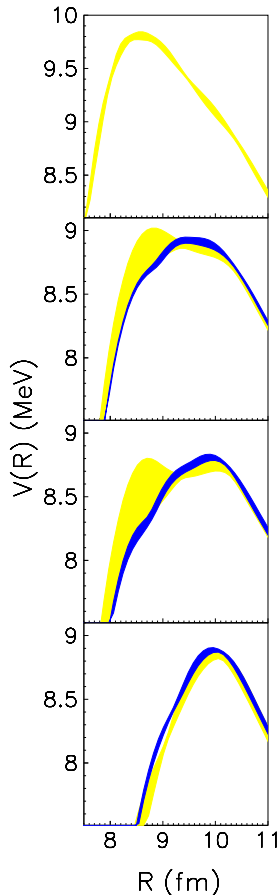


FIG. 5. Zoom of the fusion barrier region obtained for $^{16}\text{O}+^{16,22,24,28}\text{O}$ reactions respectively from top to bottom using the macroscopic interpretation of TDHF. Filled areas corresponds to calculated potential with uncertainties, the gray area corresponds to the result obtained using Eq. 2 while the black area is the result obtained including the isospin relative distance difference (see text). In the case of $^{16}\text{O}+^{16}\text{O}$ there is a simple curve since the additional degrees of freedom does not change the extracted potential.

For $^{16}\text{O}+^{22}\text{O}$ and $^{16}\text{O}+^{24}\text{O}$ reactions, rather large uncertainties are observed for specific relative distances. These uncertainties represents the dependence of the potential $V(R)$ with the initial energies, i.e. the polarisation of the extracted solution using Eq. 2 with mean-field trajectories. In our microscopic calculations, this polarisation could be directly attributed to the appearance of another important degree of freedom which is not included in Eq. 2. Indeed, regions where uncertainties are important are associated with relative distances between protons in the two nuclei differing from the distances between neutrons. In order to account for this additional effect, we have introduced the difference between the proton and neutron relative distances:

$$\Delta R_{np} = (R_1^n - R_2^n) - (R_1^p - R_2^p) \quad (13)$$

and assumed that the Eq. 2 is modified in order to include this additional degree of freedom:

$$\frac{dP}{dt} = F(R) - \gamma(R) \dot{R} - \gamma_{np}(R) \Delta \dot{R}_{np} \quad (14)$$

As in the previous case, using three different initial conditions, Eq. 14 can be interpreted as three linear equations with three unknown quantities $F(R)$, $\gamma(R)$ and $\gamma_{np}(R)$ (see Eq. A1). The inversion of such ensemble of equations is rather difficult since the additional degree of freedom is not always important during the evolution. This often leads to an overcomplete set of equations. A discussion on inversion method is given in appendix A.

Assuming that the dynamical mean-field theory can be reduced to Eq. 14, we obtain the new potentials represented by a black area in Fig. 5. In that case, the initial energy dependence are strongly reduced as compared to the previous calculation indicating the importance of this new degree of freedom. Note that in the symmetric reaction $^{16}\text{O}+^{16}\text{O}$, the additional degree of freedom can be neglected, and the obtained potential strictly corresponds to the old one. It should be noticed that the second maximum present in $^{16}\text{O}+^{22}\text{O}$ and $^{16}\text{O}+^{24}\text{O}$ reactions using Eq. 2 has disappeared. In order to quantify more precisely the effect of the neutron excess on fusion, we have fitted the new value of $V(R)$ in the vicinity of the barrier assuming $V(R) = V_B - \Delta V_B (R - R_B)^2$. We have reported in table I, the barrier height V_B , the peak position R_B and the deduced curvature $\hbar\omega_B$ defined as $\hbar\omega_B = \hbar\sqrt{\Delta V_B/\mu_0}$.

In the case of $^{16}\text{O} + ^{16}\text{O}$, where experimental data exist, a good agreement with the extracted barrier height and position [33,34] is found. For other reactions, experimental results are not available. We would like to mention that we have also applied this method to the formation of heavy and very heavy elements. In all cases, we found a good matching with the experimental fusion properties giving additional confidence in the physical meaning of the extracted barriers.

Looking at the three asymmetric reactions, the barrier height is almost constant while, as expected, the peak position increases slowly as well as the barrier diffusion. However these trends could not be extended to the symmetric case. This fact associated to the fact that it is not necessary to introduce additional degrees of freedom in the symmetric reaction case, shows the peculiarity of the neutron excess in fusion reactions.

	^{16}O	^{22}O	^{24}O	^{28}O
V_B (MeV)	9.8	8.9	8.8	8.9
R_B (fm)	8.6	9.6	9.8	10.0
$\hbar\omega_B$	2.39	1.21	1.36	1.65

TABLE I. Fusion barrier V_B and position extracted from head on collisions $^{16}\text{O}+^{16,22,24,28}\text{O}$.

In order to have some qualitative information on fusion cross sections, we have injected the values reported in table I in the Wong formula [35]:

$$\sigma_F(E) = \frac{\hbar\omega_B R_B^2}{2E} \ln(1 + \exp(2\pi(E - V_B)/\hbar\omega_B)) \quad (15)$$

where E is the laboratory energy. The cross sections for $^{16}\text{O}+^{16}\text{O}$ (thin line), $^{16}\text{O}+^{22}\text{O}$ (circles) and $^{16}\text{O}+^{28}\text{O}$ (thick line) reactions are displayed in Fig. 6. For fusion above the barrier, due to the 1 MeV lower value of the barrier, a larger fusion cross section for the case of neutron rich isotopes as compared to symmetric ^{16}O reaction is expected. However, there is no differences between ^{22}O , ^{24}O or ^{28}O above $E > 10\text{MeV}$.

The excess of neutron is also predicted to modify the sub-barrier cross-section [40,36,37]: an increase of the sub-barrier cross-section associated with a decrease of the slope of the cross-section is expected. In Fig. 6, a more complex dependence in the slope of the cross-section is observed. It should however be noted that the inclusion of friction, which is neglected in the Wong formula, may change the slope in the sub-barrier region. Since the friction changes considerably between stable and neutron rich nuclei (see Fig. 4), a comparison of the different slopes is difficult. In the case of the two reactions $^{16}\text{O}+^{22}\text{O}$ and $^{16}\text{O}+^{28}\text{O}$, friction coefficients have the same behavior as a function of the relative distance and the cross-sections may be compared. In this case, we indeed observe a smaller slope in the ^{28}O case.

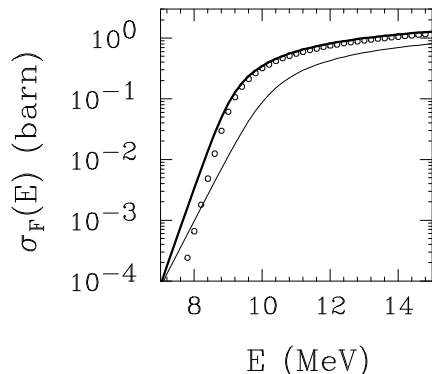


FIG. 6. Example of calculated fusion cross-section using the Wong formula for the reaction $^{16}\text{O}+^{16}\text{O}$ (thin line), $^{16}\text{O}+^{22}\text{O}$ (circles) and $^{16}\text{O}+^{28}\text{O}$ (thick line).

The evolution of $\gamma_{np}(R)$ as a function of the relative distance is shown in Fig. 7 as well as the position of the barrier. The effect of the new coordinate is intermittent. The first maximum of γ_{np} is close to the barrier. This is directly understood by the fact that, at this point, the difference between proton and neutron distances is maximum. Indeed, in this case, the coulomb repulsion is large, which goes in favour of a larger proton distance while, due to the existence of a neutron skin, the attractive nuclear part acts first on neutrons and thus tends

to reduce the neutron distance. After the contact, the effect of γ_{np} appears periodically due to the appearance of neutron-proton oscillations which are already present in the entrance channel.

The necessity to introduce explicitly the difference between neutron and proton center of mass in neutron-rich nuclei has already been noted in several work [39–41]. In all cases, it was concluded that the neutron excess is expected to increase the fusion cross-section as also observed in the present work. Different effects are indeed expected to act in this direction: the large extension of the neutron skin which implies the influence of the nuclear field at larger relative distance, the coupling between the soft dipole mode with the relative motion. The time-dependent mean-field model includes all these effects. In particular, the observable ΔR_{np} is obviously connected to the polarisation of each nucleus before fusion. It should also be noted that ΔR_{np} is affected by the transfer of particles initiated just after the contact in order to equilibrate the N/Z ratio between the two partners. This transfer which is known to induce damping in the relative motion, gives rise to the excitation of a pure collective GDR in the composite nucleus [42].

Although the additional friction term in Eq. (14) seems to strongly reduce uncertainties on the extracted potentials, for longer time, a more complex dynamics is expected. In particular, it would be convenient to treat also collective processes like the excitation of giant resonances. For instance, the effect of polarisation as well as the onset of the GDR after fusion requires the introduction of potential effect coming from the symmetry energy.

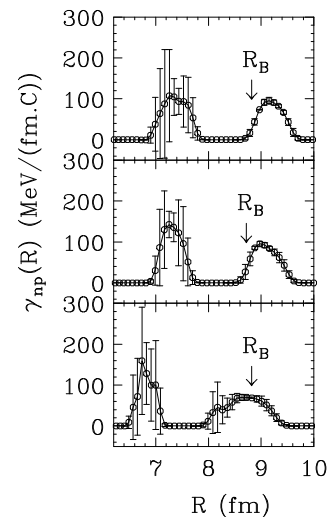


FIG. 7. Top: Friction coefficient γ_{np} as a function of the relative distance in head-on $^{16}\text{O}+^{22}\text{O}$ (top), $^{16}\text{O}+^{24}\text{O}$ (middle) and $^{16}\text{O}+^{28}\text{O}$ (bottom) reactions. The barrier position is indicated by an arrow.

To quantify the amount of energy transferred from the relative motion to the new coordinate, we have also computed a quantity similar to E_{loss} noted E_{np} which is de-

defined as:

$$E_{np}(R) = - \int_{t_0}^t \gamma_{np}(R(s)) \dot{R}(s) \Delta \dot{R}_{np}(s) ds \quad (16)$$

The result of the computation is shown in Fig. 8. The amount of transferred energy to the new observable is directly proportional to the neutron excess.

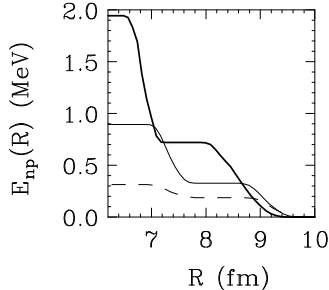


FIG. 8. Energy transferred between the relative motion and the neutron to proton oscillation as a function of the relative distance for the reaction $^{16}\text{O}+^{22}\text{O}$ (dashed line), $^{16}\text{O}+^{24}\text{O}$ (thin line) and $^{16}\text{O}+^{28}\text{O}$ (thick line).

III. CONCLUSION

In this paper, we have shown that the properties of a macroscopic dynamics can be rather precisely inferred from a microscopic quantum mean-field dynamics by reducing the one-body information to few collective coordinates. In order to have quantitative information on the barrier properties, the "naive" reduction taking into account only the relative distance is not sufficient in neutron rich nuclei and it is necessary to introduce the difference between neutrons and protons during the onset of fusion.

We have applied our method to the case of head-on oxygen reactions involving oxygen isotopes. We have shown that, while the fusion barrier is only slightly affected by the neutron skin, the barrier shapes change. We thus expect that the neutron skin will modify preferentially the sub-barrier fusion reactions.

Beside the potential landscapes, the mean-field dynamics gives also information on how the relative motion dissipates into internal excitation of the composite system. Such a dissipation which gives directly the associated friction coefficient has rarely been obtained in non-adiabatic microscopic theory. We have shown that during the initial stage of the reaction, part of the dissipation corresponds to an isospin symmetric dissipation of the relative motion (γ). In this case, the total amount of energy deposited in the system seems independent of the neutron skin. On the other side, another part of the dissipation associated with the neutron-proton difference (γ_{np}) depends explicitly on the neutron excess.

In this work, we have shown how mean-field theory which includes nuclear structure effects and does not invoke specific approximations on macroscopic dynamics, may be very useful to extract quantitative information on the potential landscapes as well as on dissipation.

The techniques developed in this paper may be of particular interest for super-heavy systems in which macroscopic theories are presently widely used [38,43–45]. There, friction coefficients are often calculated assuming thermal equilibrium of other degrees of freedom. Such an assumption is not included in TDHF and it would be desirable to compare the two approach.

Acknowledgments

The author thank Paul Bonche for helpful discussion at the initial stage of this work and for providing the three dimensional TDHF code. Usefull discussion with Cédric Simenel, Stéphane Grévy and Olivier Juillet are acknowledged. We finally thank Dominique Durand for a carefull reading of the manuscript.

APPENDIX A: INVERSION OF EQUATION WITH ΔR_{NP}

Using three TDHF trajectories, noted (I, II and III), Eq. 14 can be interpreted as a matricial equation which reads for a given position R :

$$\begin{pmatrix} 1 & -\frac{dR^I}{dt} & -\frac{d\Delta R_{np}^I}{dt} \\ 1 & -\frac{dR^{II}}{dt} & -\frac{d\Delta R_{np}^{II}}{dt} \\ 1 & -\frac{dR^{III}}{dt} & -\frac{d\Delta R_{np}^{III}}{dt} \end{pmatrix} \begin{pmatrix} F(R) \\ \gamma(R) \\ \gamma_{np}(R) \end{pmatrix} = \begin{pmatrix} \frac{dP^I}{dt} \\ \frac{dP^{II}}{dt} \\ \frac{dP^{III}}{dt} \end{pmatrix} \quad (\text{A1})$$

which we write $\mathcal{M}\mathcal{X} = \mathcal{B}$ in the following. The inversion of A1 is made difficult due to the fact that the additional degree of freedom acts intermittently on the other components. When the coupling between ΔR_{np} of freedom is small, the set of equations becomes overcomplete.

In order to solve this difficulty, we first consider two TDHF trajectories and solve the two-dimensional Eq. 10. This gives an approximative solution of A1 ($F_0(R), \gamma_0(R)$). A measure of the importance of ΔR_{np} is then obtained by computing the residue of the three dimensional equation:

$$Res(R) = \|\mathcal{M}\mathcal{X}_0 - \mathcal{B}\|^2 \quad (\text{A2})$$

where $\mathcal{X}_0 = {}^t (F_0(R), \gamma_0(R), 0)$. Example of calculated residue for the $^{16}\text{O}+^{22}\text{O}$ and $^{16}\text{O}+^{24}\text{O}$ reactions are presented in Fig. 9. We see that a large residu at a given time (or equivalently position) initiate the errors for future time (or lower position). This comes from the fact that we compute $V(R)$ by integration of F over R from large to small R values.

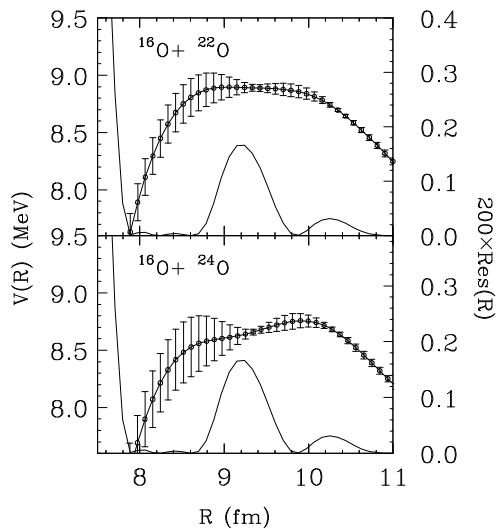


FIG. 9. Example of calculated residue for the reactions $^{16}\text{O}+^{22}\text{O}$ (top), $^{16}\text{O}+^{24}\text{O}$ (bottom) as a function of the relative distance. The potential obtained by inversion of equation 10 is also superimposed with errorbars.

In this figure, the appearance of larger and larger residues during the approaching phase towards the fused systems is clearly observed. This effect may be seen as the starting of neutron-proton oscillations. We also remark that in between the maxima, the residue is very close to zero and equation A1 reduces to Eq. 10. In our numerical implementation, when the residue is large, we solve equation A1 while for very small values, we switch to Eq. 10.

[1] W. Nörenberg and H. A. Weidenmüller, *Introduction to the Theory of Heavy-Ion Collisions*, Springer-Verlag, (1980).

[2] W. U. Schröder and J. R. Huizenga, *Treatise on Heavy-Ion Science* vol. **3** (1984) 115.

[3] P. Fröbrich and R. Lipperheide, "Theory of nuclear reactions", *Oxford University Press*, (1996) *and references therein*.

[4] Y. Abe, S. Ayik, P. G. Reinhard and E. Suraud, *Phys. Rep.* **275** (1996) 49.

[5] H. Hofmann, *Phys. Rep.* **284** (97) 137.

[6] P. Ring and P. Schuck, *The Nuclear Many-Body Problem*, *Spring-Verlag*, New-York (1980).

[7] P. Bonche, S. Koonin and J.W. Negele, *Phys. Rev.* **C13** (1976) 1226.

[8] J.W. Negele, *Rev. Mod. Phys.* **54** (1982) 913.

[9] K.T.R. Davies, K.R.S. Devi, S.E. Koonin, and M. Strayer, *Treatise in Heavy Ion Sciences*, vol. **4**; *Nuclear Sciences*, edited by D.A. Bromley (Plenum, New York-1984).

[10] P. Fröbrich and I.I. Gontchar, *Phys. Rep.* **292** (1998) 131.

[11] H.A. Weidenmüller, *Progress in Nuclear and Particle Physics* **3** (1980) 49.

[12] G. Giardina, F. Hanappe, A.I. Muminov, A.K. Nasirov and L. Stuggè, *Nucl. Phys.* **A671** (2000) 165.
G. Giardina, S. Hofmann, A. I. Muminov and A. K. Nasirov, *Eur. Phys. J.* **A8** (2000) 205

[13] W.J. Swiatecki, *Nucl. Phys.* **A428** (1984) 199c.

[14] U. Mosel, *Heavy Ion Collisions*, vol. 2 (1980), p. 275

[15] D.H.E. Gross, *Nucl. Phys.* **A240** (1975) 472 (*and ref. therein*).

[16] W. Bauer, D. McGrew, V. Zelevinsky and P. Schuck, *Nucl. Phys.* **A583**, 93c.

[17] B. Borderie, *Ann.Phys.(Paris)* **17**, (1992) 349

[18] S.E. Koonin, *Progress in Particle and Nuclear Physics*, **4** (1979) 283.

[19] K.-H. Kim, T. Otsuka and P. Bonche, *Journal of Phys.* **G23** (1997) 1267.

[20] E. Chabanat, P. Bonche, P. Hansel, J. Meyer and R. Schaeffer, *Phys. Scr.* **T 56** (1995) 31.

[21] E. Chabanat, P. Bonche, P. Haensel, J. Meyer and R. Schaeffer, *Nucl. Phys.* **A627** (1997) 710; *Nucl. Phys.* **A635** (1997) 231. Erratum: *Nucl. Phys.* **A643** (1998) 441.

[22] R.W. Hasse and W.D. Myers, "Geometrical Relationships of Macroscopic Nuclear Physics", Ed. Springer-Verlag, 1988.

[23] A. Bonasera, G.F. Bertsch and E.N. El-Sayed, *Phys. Lett.* **141B** (1984) 9.

[24] S.E. Koonin, K.T.R. Davies, V. Mahrun-Rezwani, H. Feldmeier, S.J. Kreiger and J. W. Negele, *Phys. Rev.* **C15** (1977) 1359.

[25] D.M. Brink and Fl. Stancu, *Phys. Rev.* **C24** (1981) 144.

[26] F.H. Jorgensen, T. Dossing, B.S. Nilsson and J. Randrup, *Phys. Lett.* **B191** (1987) 323.

[27] S. Pal and D.H.E. Gross, *Z. Phys.* **A329** (1988) 349.

[28] A. Ozawa, T. Suzuki and I. Tanihata, *Nucl. Phys.* **A693** (2001) 32.

[29] J.A. Chrisley, C. H. Dasso, S.M. Lenzi, M.A. Nagarajan and A. Vitturi, *Nucl. Phys.* **A587** (1995) 390.

[30] K.-H. Kim, T. Otsuka and M. Tohyama, *Phys. Rev.* **C50** (1994) R566.

[31] J. Blocki, Y. Boneh, J.R. Nix, J. Randrup, A.J. Sierk and W.J. Swiatecki, *Ann. Phys.* **113** (1978) 330.

[32] J. Randrup and W. J. Swiatecki, *Ann. Phys.* **125** (1980) 193.

[33] L.C. Vaz, J.M. Alexander and G.R. Satchler, *Phys. Rep.* **65** (1981) 373.

[34] Q. Haider and B. Cujec, *Nucl. Phys.* **A429** (1984) 116.

[35] C. Y. Wong, *Phys. Rev. Lett.* **31** (1973) 766.

[36] N. Takigawa and H. Sagawa, *Phys. Lett.* **B265** (1991) 23.

[37] J.-L. Sida *et al*, *Nucl. Phys.* **A685** (2001) 51c.

[38] P. Möller, J.R. Nix, P. Ambruster, S. Hofmann and G. Müzenberg, *Z. Phys.* **A359** (1997) 251.

[39] G. R. Satchler, K. W. McVoy, M.S. Hussein, *Nucl. Phys.* **A522** (1991) 621.

[40] C.H. Dasso and R. Donangelo, *Phys. Lett.* **B276** (1992) 1.

[41] L.F.Canto, R.Donangelo, P.Lotti, M.S.Hussein, *Phys.Rev.* **C52**, (1995) R2848.

- [42] C. Simenel, Ph. Chomaz and G. De France, Phys. Rev. Lett. 86 (2001) 2971.
- [43] Y. Aritomo, T. Wada, M. Ohta and Y. Abe, Phys. Rev. **C59** (1999) 796.
- [44] G.G. Adamian, N.V. Antonenko, S. P. Ivanova and W. Scheid, Nucl. Phys. **A646** (1999) 29.
- [45] R. Smolańczuk, Phys. Rev. **C59** (1999) 2634.